Cellulose
https://doi.org/10.1007/s10570-024-05945-2

ORIGINAL RESEARCH

Local water management in cotton linter papers with silica-based coatings

Joanna J. Mikolei · Markus Biesalski · Marcelo Ceolin · Annette Andrieu-Brunsen

Received: 26 January 2024 / Accepted: 4 May 2024

Abstract Paper with its mechanical strength as well as due to its microfluidic properties has emerged as an interesting sustainable material for future high-tech applications. Examples include paper-based sensors and actuators, paper-based construction materials and paper-based membranes. These examples have in common that a precise control of the water distribution inside the paper sheet during fluid water imbibition, water vapor adsorption, or drying affects the fluidic properties of the paper, which are crucial for its performance. Here silica-based coatings are applied to control the water distribution in the paper sheet during imbibition, adsorption and drying. By using dense silica coatings, the fibers are shielded from water penetration which limits the water distribution into the fiber–fiber voids. Whereas with a mesoporous silica coating, mesopores can be inserted into the paper, providing an additional space for water imbibition and adsorption. Water location upon imbibition, adsorption and drying were investigated using small angle x-ray scattering and gravimetric water vapor adsorption. Thereby, water distribution upon imbibition and adsorption depends on the type of silica coating. In addition, the drying mechanism and water distribution during drying is as well determined by the silica-based coating. The obtained results allow to deduce design criteria for local water management in paper sheets.

Supplementary Information The online version contains supplementary material available at https://doi.org/10.1007/s10570-024-05945-2.

J. J. Mikolei · A. Andrieu-Brunsen (✉)
Ernst-Berl Institut Für Technische Und Makromolekulare Chemie, Macromolecular Chemistry – Smart Membranes, Technische Universität Darmstadt, Peter-Grünberg-Straße 8, 64287 Darmstadt, Germany
e-mail: annette.andrieu-brunsen@tu-darmstadt.de

M. Biesalski
Ernst-Berl Institut Für Technische Und Makromolekulare Chemie, Macromolecular and Paper Chemistry, Technische Universität Darmstadt, Peter-Grünberg-Straße 8, 64287 Darmstadt, Germany

M. Ceolin
Instituto de Investigaciones Fisicoquímicas Teóricas y Aplicadas, Universidad Nacional de La Plata and CONICET, Diag. 113 y 64 (1900), La Plata, Argentina

Published online: 14 May 2024

Graphical Abstract

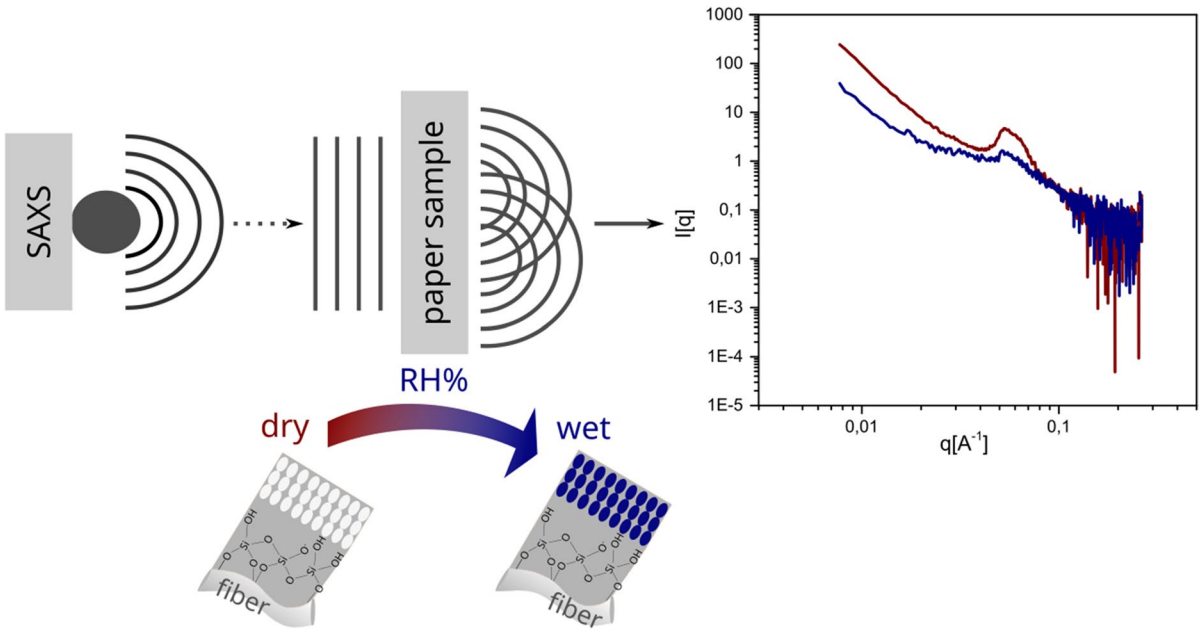

Keywords Microfluidic · Cotton Linter Paper · Silica Coatings · Nanopores · Water Condensation and Drying

Introduction

In the recent years paper-based materials underwent a transformation from a simple consumer material such as tissue paper or graphic paper toward a possible and future use as high-tech materials for construction, smart packaging, sensing, or actuator for soft robotics (Liu et al. 2021; Venkatesan et al. 2023; Li et al. 2019). The latter is driven by a rich and broad property-profile of paper which originates from a chemical complex and hierarchical paper fiber structure. Cotton linter fibers, for example, are 1 – 3 mm long and 10 – 50 µm wide. They consist of macrofibrils (length > 2 µm; width > 15 nm), which in turn are composed of bundled microfibrils with a length larger than 2 µm and a width between 5–10 nm. These microfibrils contain cellulose chains with a length less than 1 µm and a width between 1.5 – 3.5 nm (Fig. 1) (Zhu et al. 2013, Zhu et al. 2023, Li et al. 2021). Due to this structural organization as well as the hydrogen bonds between the fibers, cellulose-based materials are mechanically highly stable. In addition, fluid can be taken up and transported by capillary forces (Lee et al. 2016, Bedane et al. 2016, Dano and Bourque 2009, Chen et al. 2022, Klemm et al. 2005) Thereby, water uptake significantly affects the mechanical stability, as water screens the hydrogen bonds, causes fiber swelling, and can finally debond individual fibers which leads to a disintegration of the paper sheet. Paper intrinsic transport properties open the possibility for unidirectional moisture delivery which is of relevance for paper as a construction material or for paper in packaging applications (Shi et al. 2023, Bordenave et al. 2007). Fiber swelling and the related material expansion make paper a promising material for sustainable moisture-responsive actuators (Liu et al. 2021, Lee et al. 2016, Chen et al. 2022, Ryu et al. 2020). Up to now, the water distribution inside the paper on the fiber level is not well understood, although it is essential for the paper mechanical stability, fluid transport, and fiber swelling.

It has been reported that paper cellulose fibers adsorb water from water vapor (Sinquefield et al. 2020). Adsorbed water vapor or imbibed liquid water is classified into ‘free-’ and ‘bound-water’ (Weise

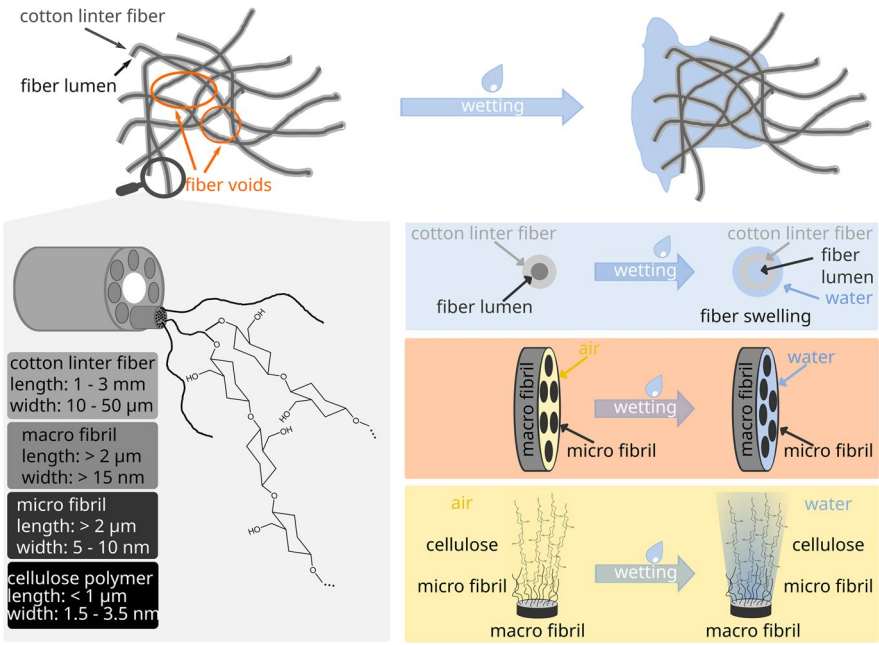

Fig. 1 Possible water location in unmodified cotton linter paper sheets upon complete wetting in contact with liquid water

et al. 1996, Samyn 2013, Bechtold et al. 2013). The bound water is subdivided into 'freezing-' and 'non-freezing-water' (Nakamura et al. 1981). This classification is based on the water location within the paper and its physical or chemical interaction with the cellulose fiber (Samyn 2013). 'Free-water' is located between the fibers, in the fiber lumen as well as in the pores of the fiber wall and forms no hydrogen bond with the hydroxyl groups of the fiber (Samyn 2013). 'Freezing-' and 'non-freezing water' instead is located close to the fiber surface and in the pores of the fiber wall (Samyn 2013, Nakamura et al. 1981). Thereby, 'non-freezing water' forms hydrogen bonds with the hydroxyl groups of the cellulose polymer chain which prevents the water from freezing. Below a critical pore size of 4 nm only 'non-freezing water' exist. Whereas in pores with a large size both bound water types, freezing and non-freezing water, have been reported (Nakamura et al. 1981). Mainly differential thermal calorimetry (DSC), nuclear magnetic resonance (NMR) or near-infrared hyperspectral imaging (NIR) are used to distinguish between 'free-' and 'bound-water' (Weise et al. 1996, Lovikka et al. 2018, Kaewnopparat et al. 2008, Heikkinen et al. 2006, Ogiwara et al. 1970, Ma et al. 2020). NIR imaging turned out to be a promising method to visualize the drying process. By using NIR imaging Ma et al. were able to follow the drying process in lignocellulosic materials and to visualize changes in the water distribution of 'free-' as well 'bound-water' during drying (Ma et al. 2020). Analytical techniques used to date in this context, however, do not allow to extract information on the fiber structure during swelling and deswelling upon wetting and drying. Small Angle X-Ray Scattering (SAXS) enables the hierarchical structure of cellulose fibers containing nanoscale sized units to be investigated under different ambient conditions (Martínez-Sanz et al. 2015). Penttilä et al. as well as Larsson et al. proposed analytic models for modelling SAXS data recorded from cellulose-based materials under dry and wet conditions with respect to the arrangement of the fibrils inside the cellulose fiber (Penttilä et al. 2019, Larsson et al. 2022).

Independently of the location of the water, the water amount decreases with increasing number of drying and rewetting steps (Weise et al. 1996, Samyn 2013). Jayme et al. explained this decrease in water amount upon drying and rewetting with a change in the fiber structure which they named hornification (Jayme 1944; Jayme and Hunger 1956). Lovikka et al. showed that during this hornification the fiber specific surface area decreases due to a collapse of the fiber intrinsic mesopores (Lovikka et al. 2016). Consequently, less water is adsorbed within subsequent water adsorption cycles upon increasing the

humidity (Lovikka et al. 2018, Lovikka et al. 2016). The change in the amount of adsorbed water due to the several drying and rewetting steps is expected also to influence the deformability of the paper due to less fiber swelling upon drying and rewetting, which impacts, for example, the motion of an actuator.

Here we present the first insights into local water distribution at the cellulose chain, the microfibril and the cellulose polymer during wetting and drying of model cotton linters paper sheets using SAXS. We show the possibility to tune the local water distribution by suppressing fiber swelling due to the control of 'free-' and 'bound-water' using different silica coatings on the paper fibers. Three different silica functionalization dependent drying mechanisms were observed. Silica-based coatings enable precise local water management in cotton linter papers which is of high-tech paper materials with possible applications as constructing material, smart packaging or as stimuli-responsive actuators.

Materials and Methods

Reagents

All chemicals and solvents were purchased from Merck and used as received.

Paper Fabrication

For the preparation of lab-engineered paper substrates cotton linter fibers (curl: 18.7%, fibrillation degree: 1.6%, fines content: 37.1%) were used which were provided by the Eifeltor Mühle factory. The cotton linter pulp was refined in a Voith LR 40 laboratory refiner with an effective specific energy of 200 kWh t^{-1}. From these pulp lab-engineered paper sheets with a grammage of 50 – 53 g m^{-2} were fabricated using a conventional Rapid-Koethen hand sheet maker according to DIN 54358 and ISO 5269/2 in absence of additives and fillers.

Dense and Mesoporous Sol–Gel Solutions

To prepare a mesoporous silica coating at cotton linter papers, a sol–gel solution containing TEOS as precursor and the micelle forming template Pluronic® F127 was prepared with the following molar ratios: 1 TEOS:20 EtOH: 0.05 F127: 5 H2O: 0.01 conc. HCl. A dense silica coating was realized with the same chemicals in the same ratio but in the absence of the template F127. Before use, the freshly prepared sol–gel solution was stirred for 24 h at room temperature.

Paper Functionalization

Dip coating was used to apply the silica in contact with fibers. Cotton linter papers with a length of 6 cm and a width of 2 cm were dipped into the sol–gel solution and withdrawn at a speed of 2 mm s^{-1}. The dip-coating procedure was performed at a relative humidity of $50 \pm 5\%$ and a temperature of 25 ± 1 °C. To develop a mesoporous silica coating on the fiber, the samples were dipped in a sol–gel solution which contains the micelle forming template Pluronic® F127. For a dense silica coating on the fibers, the papers samples were dipped in a sol–gel solution without the micelle forming template. After dip coating, the cotton linter papers with a mesoporous silica coating were first aged for 1 h under the same humidity and temperature before undergoing thermal post-treatment. To form a dense silica coating aging was omitted and the samples were underwent thermal post-treatment directly. The post thermal treatment consisted of raising the sample temperature first to 60 °C in 10 min and then held at that temperature for 1 h followed by another increase of the temperature to 130 °C in 10 min. The final sample temperature of 130 °C was kept for 1 h before cooling down to room temperature. To remove template in the case of the mesoporous silica coating, an extraction was made in a 1 m acidic ethanol bath for 3 days.

Small Angle X-Ray Acattering (SAXS)

Most of the SAXS experiments were performed in a XEUSS 1.0 SAXS setup (XENOCS, Grenoble, France). Monochromatic X-rays ($\lambda = 0.15419$ nm) were produced with a GENIX 3D micro-focus tube. The incoming X-ray beam was collimated to have a size at sample position of 0.5×0.5 mm^2. Scattered photons were detected using a PILATUS 100 K detector placed at $D = 2500$ mm sample to detector distance (calibrated using Silver Behenate as standard). For following the drying and the wetting process, a square paper samples with a dimension of

2.25 cm^2 was placed in a chamber with controlled humidity. A 15 µL water droplet was placed onto the paper sample and the SAXS measurements were started immediately after putting the drop. The drying process was followed for 15 min, recording one SAXS diagram every minute. Along the experiment, the relative humidity was set to 50 ± 5% using a humidity controller. Temperature of the samples were kept at 25 °C along all the experiments. Before starting every experiment, paper samples were dried at 100 °C for 1 h. Ultra low SAXS experiments (USAXS) were performed at the CATERETE beam line of the SIRIUS accelerator (Campinas, Brazil) as part of the project 20220451. The X-ray beam energy was at to 10 keV ($\lambda = 0.1239$ nm) and the sample-to-detector distance was either 28 m or 10 m (depending on q-range). X-ray beam attenuation was calculated using the signal available from a pin-diode placed in front of the scattering detector normalized to the count rate obtained in the absence of sample (around 20000 counts per sec) (see Figure S1).

Vapor Sorption

Moisture sorption was measured using the SPSx-1µ Advance form ProUmid (ProUmid GmbH, Ulm, Germany). Samples with a disk shape and a diameter of 2.5 cm underwent adsorption (0% to 90% in 10% steps) and desorption (80% to 0% in 10% steps) at 25 °C. The overall measuring time was 4 days with an equilibration time of 40 min for each relative humidity. For the evaluation of the moisture sorption measurements, the sample weight was plotted against the corresponding humidity after reaching equilibrium.

Results and Discussion

Structural changes and water distribution inside cotton linter papers upon drying with and without silica functionalization

To investigate the drying and wetting processes in cotton linter paper as well as the water distribution upon condensation in dependence of the relative humidity, cotton linter paper sheets were modified with dense and mesoporous silica coatings. To obtain a mesoporous silica coating, a paper sheet was dip coated into a sol–gel solution containing the mesopore forming template Pluronic® F127 and the silica precursor TEOS. Dense silica coatings were realized using TEOS in acidic ethanol without adding mesopore forming template. Dip-coating was performed at a relative humidity of 50% ± 5% and a temperature of 25 °C ± 1 °C. The control of the environmental conditions is of great importance because the evaporation induced self-assembly of the mesopore forming template is highly affected by the solvent evaporation rate, the template concentration, and the paper intrinsic fluid transport velocity as we demonstrated in a previous study (Mikolei et al. 2022, Mikolei et al. 2023). After dip-coating the paper sheet was aged for one hour under the environmental conditions used for dip-coating followed by a thermal post-treatment with the final temperature of 130 °C. The thermal post-treatment facilitates the hydrolysis and condensation reaction of the silane precursor and thus silica network formation. For the mesoporous silica coating the template was extracted after the thermal post-treatment using a 0.01 M acidic ethanol bath for 3 days.

When completely wetting cotton linter paper sheets, water can be located within the fibers (Fig. 1 lower part) as well as between the fibers (Fig. 1 upper part). Water being located within the fibers can be located within the different structural units of a fiber such as the lumen or the macro-, or micro fibrils. SAXS measurements allow to distinguish between water being located within the micro fibril and the cellulose polymer. Thus, a precise understanding of water distribution at the fiber level can be obtained.

In order to discuss the SAXS results obtained from paper samples, both, during water uptake and release, SAXS diagrams were normalized to take into account the changes in signal attenuation due to the presence of water inside the paper structure (following the procedure described in the secton Materials and Methods). Beyond the attenuation produced by water into X-ray beam, the temporal evolution of the water content forces us to take into account the differential effects on the attenuation of the beam. In order to verify our models, the attenuation obtained for fully wet samples (0.3) was in fair agreement with the value calculated using a linear combination of the attenuation calculated for pure cellulose and water assuming a 12% w/w amount of water (0.31). Calculations were performed using the algorithm implemented by The Center of X-ray

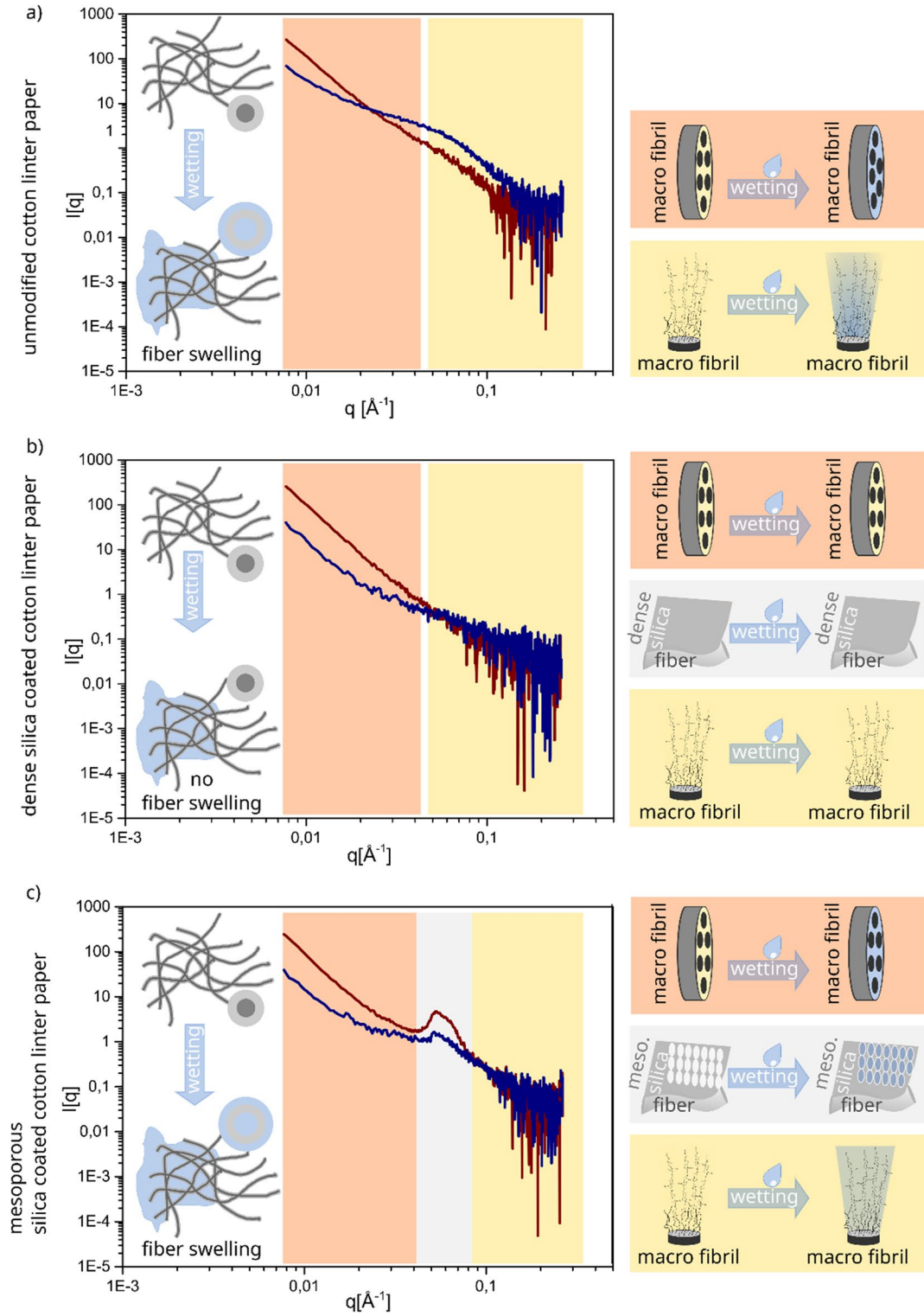
a)
unmodified cotton linter paper
I[q]
q [Å^{-1}]
wetting
fiber swelling
macro fibril
macro fibril
wetting
wetting
macro fibril
macro fibril
b)
dense silica coated cotton linter paper
I[q]
q[Å^{-1}]
wetting
no
fiber swelling
macro fibril
macro fibril
wetting
dense
silica
fiber
dense
silica
fiber
wetting
macro fibril
macro fibril
c)
mesoporous
silica coated cotton linter paper
I[q]
q[Å^{-1}]
wetting
fiber swelling
macro fibril
macro fibril
wetting
meso.
silica
fiber
meso.
silica
fiber
wetting
macro fibril
macro fibril

◂**Fig. 2** **a** SAXS measurements of unmodified cotton linter paper in dry and wet state with the correlation of the water location on microfibril and cellulose polymer size range. **b** SAXS measurement of dry and wet dense silica coated cotton linter paper, showing the shielding property of the dense silica coating which hinders water to penetrate the fibers. **c** SAXS measurements of cotton linter paper with mesoporous silica coating in dry and wet stay, showing that water is located at the complete fiber and enters the pores of the coating

Optics (https://henke.lbl.gov/optical_constants/filter2.html). Figure S1 also shows a typical attenuation curve corresponding to the drying of unmodified paper. Hereinafter, SAXS results should be interpreted as attenuation normalized SAXS results.

The SAXS measurements of unmodified, dry cotton linter papers show a constant intensity decrease in the range between 0.08 nm^{-1} and 3 nm^{-1} (Fig. 2 a red). This range in scattering vector is correlated to structures with a size between 2 and 80 nm, which corresponds to microfibrils and the cellulose polymer in the cotton linter paper (Fig. 2 a red). The constant decrease of the intensity with increasing scattering angle indicates the absence of any preferential orientations of the cellulose polymer and the microfibrils inside the unmodified cotton linter paper under dry conditions. Upon wetting a 2.25 cm^2 cotton linter paper sheet with a 15 µL water droplet, two main changes in the SAXS measurement as compared to the dry state (Fig. 2 a blue) are observed: firstly, in the low q region (below 0.02 $Å^{-1}$) the intensity decreased with increasing scattering angle as a result of the contrast reduction due to the filling of the fiber–fiber voids and the intersection between the microfibrils inside the macrofibril with so-called free-water (Figure S2) (Weise et al. 1996, Samyn 2013); secondly, in the high q region, above 0.02 $Å^{-1}$, an intensity increase with increasing scattering angle was observed indicating an increase in the contrast due to the interplay of the so-called bound water with the cellulose polymers and the swelling of the microfibrils (Fig. 2 a blue) (Weise et al. 1996, Samyn 2013). Consequently, SAXS data of unmodified cotton linter papers show that upon contact with liquid water the voids between the cotton linter fibers as well as the intersection between the microfibril are filled with water. Resulting in swelling of the macrofibrils and an interaction between the water and the cellulose polymer occurs.

Interestingly, no structural changes were detected, when comparting dry dense silica-coated with the unmodified, dry cotton linter paper. The intensity of the SAXS data decreases with increasing scattering angle as observed for the unmodified cotton linter paper (Fig. 2 b red). Immediately after wetting with a 15 µL water droplet the dense silica coated paper sheet, the SAXS diagram show a constant decrease in the intensity along the complete scattering angle range. Thereby, the intensity of the SAXS measurement from the wet sample is lower in the range of 0.08 to 0.03 $Å^{-1}$ due to the presence of 'free-water' (Fig. 2 b red and blue). For a q value of 0.04 $Å^{-1}$ and with further increasing scattering angle identical SAXS data are observed for dry and wet dense silica coated cotton linter paper. This is caused by an equal contrast which indicates the absence of interaction between water and the cellulose polymer as well the absence of fiber swelling. Consequently, the dense silica coating seems to shield the cellulose fibers from water penetration and thus prevents the swelling of the cellulose fibers. Accordingly, no 'bound-water' was detected and water is exclusively located in the fiber–fiber voids as 'free-water' (Fig. 2 b). This observation by SAXS is in accordance with characterization of liquid water imbibition by confocal laser scanning microscopy (CLSM) indicating water only in the fiber–fiber voids and the suppression of fiber swelling when applying a dense silica coating at the cotton linter paper as we investigated in our previous studies (Mikolei et al. 2022).

Mesoporous silica coated; dry cotton linter paper shows a Bragg peak at 0.05 $Å^{-1}$ which is attributed to the regularly arranged mesopores. A mesopore distance of ~ 12.3 nm has been deduced (Fig. 2 c red) and already described in our previous study (Mikolei et al. 2023). When wetting the mesoporous silica coated paper with water, the fiber–fiber voids are filled with 'free-water' as well as with 'bound-water' which interacts with the cellulose polymer and also fiber swelling occurs. The presence of 'free-water' and 'bound-water' are indicated by the reduced intensity of the SAXS measurement for scattering angles larger than 0.04 $Å^{-1}$ and the slight increase in the intensity at scattering angle larger than 0.03 $Å^{-1}$ as compared to the dry mesoporous silica coated sample (Fig. 2 c blue). In addition, water is present within the mesopores as indicated by the decreased intensity of the Bragg peak due

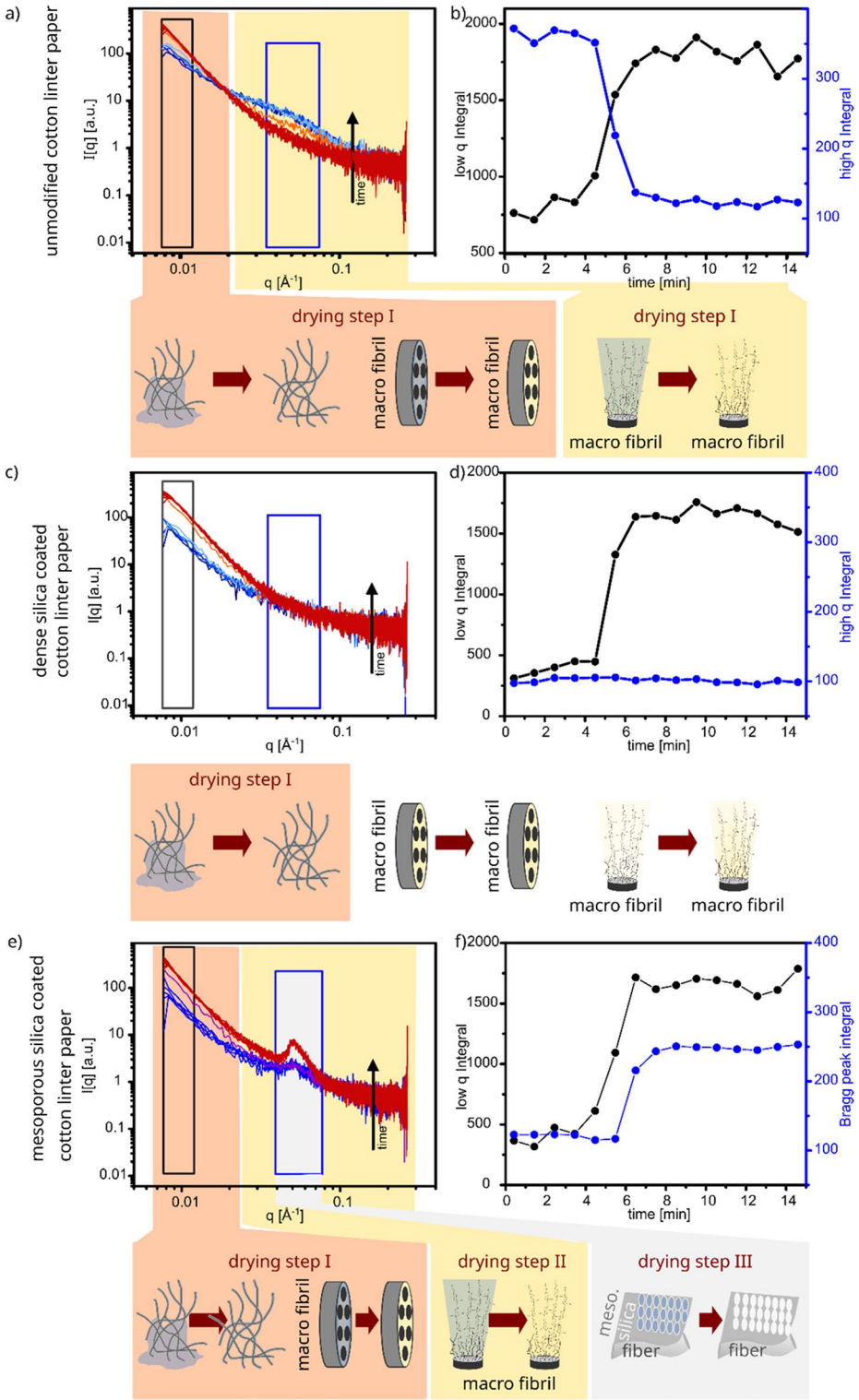
a)
unmodified cotton linter paper
I[q] [a.u.]
q [Å⁻¹]
time
b)
low q Integral
high q Integral
time [min]
drying step I
macro fibril
macro fibril
drying step I
macro fibril
macro fibril
c)
dense silica coated cotton linter paper
I[q] [a.u.]
q [Å⁻¹]
time
d)
low q Integral
high q Integral
time [min]
drying step I
macro fibril
macro fibril
macro fibril
macro fibril
e)
mesoporous silica coated cotton linter paper
I[q] [a.u.]
q [Å⁻¹]
time
f)
low q Integral
Bragg peak integral
time [min]
drying step I
macro fibril
drying step II
macro fibril
drying step III
meso. silica
fiber
fiber

◂**Fig. 3** SAXS measurements of unmodified cotton linter paper (**a**), dense silica (**c**) and mesoporous silica coated paper (**e**) which were taken during the drying process every minute for 15 min. In the upper part of the SAXS measurements the correlated fiber structure units are mentioned. Gray and blue boxes indicate the area from which the integrals were determined for integral depended illustration of the drying process from unmodified (**b**), dense silica (**d**) and mesoporous silica coated cotton linter paper (**f**)

to electronic density matching. In the following, the water inside the mesopores of the silica coating (Fig. 2 c), is called 'mesopore-water'.

In addition to the fluid water distribution, the three differently silica-functionalized paper sheets differ in their drying mechanisms due to the varying water distribution. To investigate the drying process, the completely wetted, unmodified cotton linter paper sheets and the dense- as well as the mesoporous silica coated cotton linter paper sheets (1.5×1.5 cm^2) were characterized upon increasing drying time using SAXS in transmission mode. A first SAXS measurement was recorded directly after the 15 µL water deposition as well as every minute up to 15 min. To ensure constant conditions, the measurements were performed at a relative humidity of $50\% \pm 5\%$ and a temperature of 25 °C ± 1 °C. Unmodified and mesoporous silica coated cotton linter paper sheets show a two-step drying process: first the so-called 'free-water' evaporates, subsequently the 'bound-water' evaporates in the second step (Fig. 3 a, and e). Dense silica coated cotton linter papers, which only contain free water, show a one-step drying process upon evaporation of the so-called 'free-water' (Fig. 3 c). The first step within the drying process of removing the 'free-water' seems to be identical for all paper sheets independently of their modification. Thereby, water evaporation is deduced from the intensity increase for scattering angles below 0.04 Å^{-1} until the scattering intensity adapts to the SAXS curve of the dry paper (Fig. 3 a, c, and e). This is observed after 7 min of drying independently of the paper modification (Fig. 3 b, d, and f). While drying, the integral of the area below the SAXS intensity measurement curve, representing the 'free-water' (Fig. 3 a, c, and e black box), increases due to the evaporation of the 'free-water'. The strongest increase in the integral intensity occurs between 4 and 7 min. After 8 min a complete removal of the 'free-water' was observed which is reflected in a nearly constant value of the integral (Fig. 3 b, d, and f black box).

The second step of the drying process is ascribed to the evaporation of so-called 'bound-water' and is thus only observed for unmodified and mesoporous silica coated paper sheets (Fig. 3 a, b, e, and f). Thereby, the intensity of the SAXS measurement in the scattering angle larger than 0.04 Å^{-1} decreased for drying times longer than 7 min until the SAXS measurement for a dry sample is reproduced (Fig. 3 a, and e). For unmodified paper as well the integral intensity which represents the 'bound-water' decreases (Fig. 3 b blue) after 5 min of drying. The 'bound-water' in unmodified paper is fully removed after 8 min indicated by reaching a constant value of the integral depicting the 'bound-water'. In mesopores silica coated paper sheets the 'mesopore-water' evaporates together with the 'bound-water' during this second drying step. Due to the overlapping areas ascribed to the mesopores inside the coating (Bragg-Peak at 0.05 Å^{-1}) and the cellulose polymer (scattering angle larger 0.04 Å^{-1}) in the SAXS measurement, the removal of 'bound-' and 'mesopore-water' cannot be totally distinguished in mesopores silica coated papers. The evaporation of the 'mesopore-water' is represented by the increase in the intensity of the Bragg peak upon drying. Due to the decrease in the electron density inside the pores which results in a higher contrast and is clearly shown in the increase of the integral representing the 'mesopore-water' after 6 min of drying under the applied conditions (Fig. 3 e, and f).

The observed different water types in cotton linter paper sheets and the step wise evaporation of these different water types clearly underline the influence of the hierarchical paper structure and indicates possibilities for humidity-dependent local water management in paper sheets.

Water vapor adsorption in different silica coated cotton linter paper

Besides controlling fluid water distribution in paper, water management in paper sheets needs understanding and regulation of local water vapor adsorption and condensation. Interestingly SAXS measurements of unmodified and dense silica coated paper sheets at 95% relative humidity do not show structural changes which are correlated to 'free-' and 'bound-water' (Figure S3). This is unexpected because with gravimetric water vapor adsorption weight gain starting at 10% relative humidity is detected. At a relative

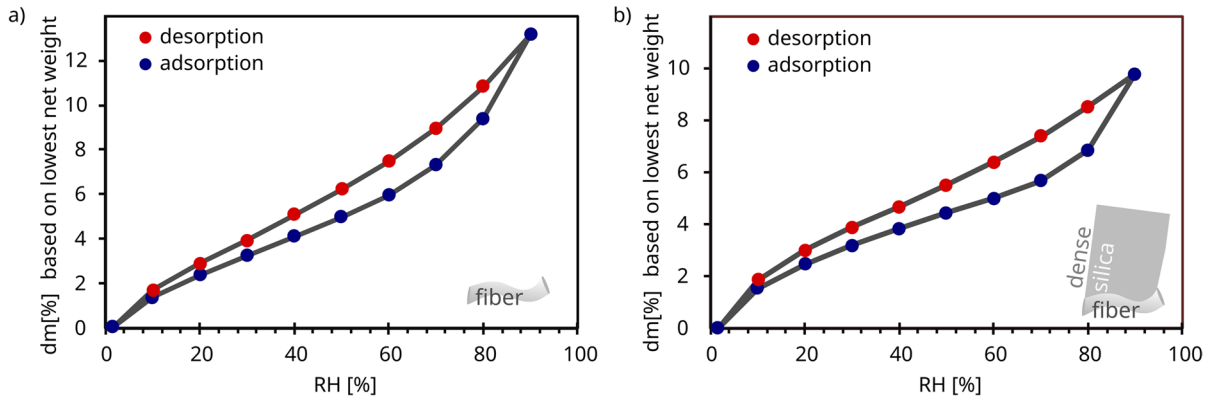

Fig. 4 Water vapor adsorption (red circles) and desorption (blue circles) isotherms in the range of 0% to 90% relative humidity for unmodified (**a**) and dense silica coated (**b**) cotton linter paper

humidity of 50% a total weight gain of 5 wt% for unmodified and 4 wt% for dense silica coated papers as compared to the dry sample weight is obtained (Fig. 4 a and b). By increasing the relative humidity from 50 to 90% a total weight gain of 13 wt% for unmodified and 10 wt% for dense silica coated paper was detected (Fig. 4). Thereby, the different amount of adsorbed water may have different origins. It may be affected by the provided surface area. Unmodified cotton linter paper has a specific surface area of 1.2 $m^2\ g^{-1}$, which is slightly larger than the specific surface area of 1 $m^2\ g^{-1}$ for dense silica cotton linter paper sheets for unmodified cotton linter (Mikolei et al. 2023). Another explanation might be the suppression of fiber swelling and thus the absence of 'bound-water' and different water locations within the paper sheet due to the dense silica coating. For unmodified as well as with dense silica coated paper the amount of adsorbed water at a relative humidity of 95% is not sufficient to obtain structural changes visible by SAXS corresponding to 'free-' or 'bound-water' (Figure S3).

Using SAXS the condensation of water vapor into the mesopores and thus the formation of 'mesopore-water' in mesoporous silica coated paper sheets is observed (Fig. 5 a). At a relative humidity of 50% condensation of water vapor into the mesopores starts as deduced from the Bragg peak intensity decrease at 0.05 $Å^{-1}$. Because of the higher electron density resulting in contrast matching due to the water condensation inside the mesopores of the silica coating a Bragg peak intensity decrease is observed. With a further increase of the relative humidity above 50% water continues condensing into the mesopores until completely filled mesopores are obtained, which results in the almost complete disappearance of the Bragg peak due to index matching at the relative humidity of 90% (Fig. 5 a). It must be noted that no change in the integral intensity of the Bragg peak was observed over time by keeping a specific relative humidity of 50%, 75% or 85% for 30 min (Fig. 5 d) indicating that the water adsorption and condensation into the mesopores is faster than the duration of the experiment.

The formation of only 'mesopore-water' by increasing the relative humidity is clearly confirmed through the decrease of the integrals below the Bragg peak (Fig. 5 b blue) while the integral related to 'free-water' stays constant indicating the absence of 'free-water' for increasing relative humidity (Fig. 5 b black). In addition to 'mesopore-water' the water content in the paper increases due to water vapor adsorption which results in a total weight gain of 5 wt% at a relative humidity of 50% and 11 wt% at the relative humidity to 90% (Fig. 5 c). This total weight gain is slightly below the one for unmodified cotton linter paper of 13 wt% (Fig. 4 a, and 5 c), even though mesoporous silica coated papers have additional 'mesoporous-water'. Also, the specific surface area of mesoporous silica coated cotton linter paper is 13-times larger than the one for unmodified paper (Mikolei et al. 2023).

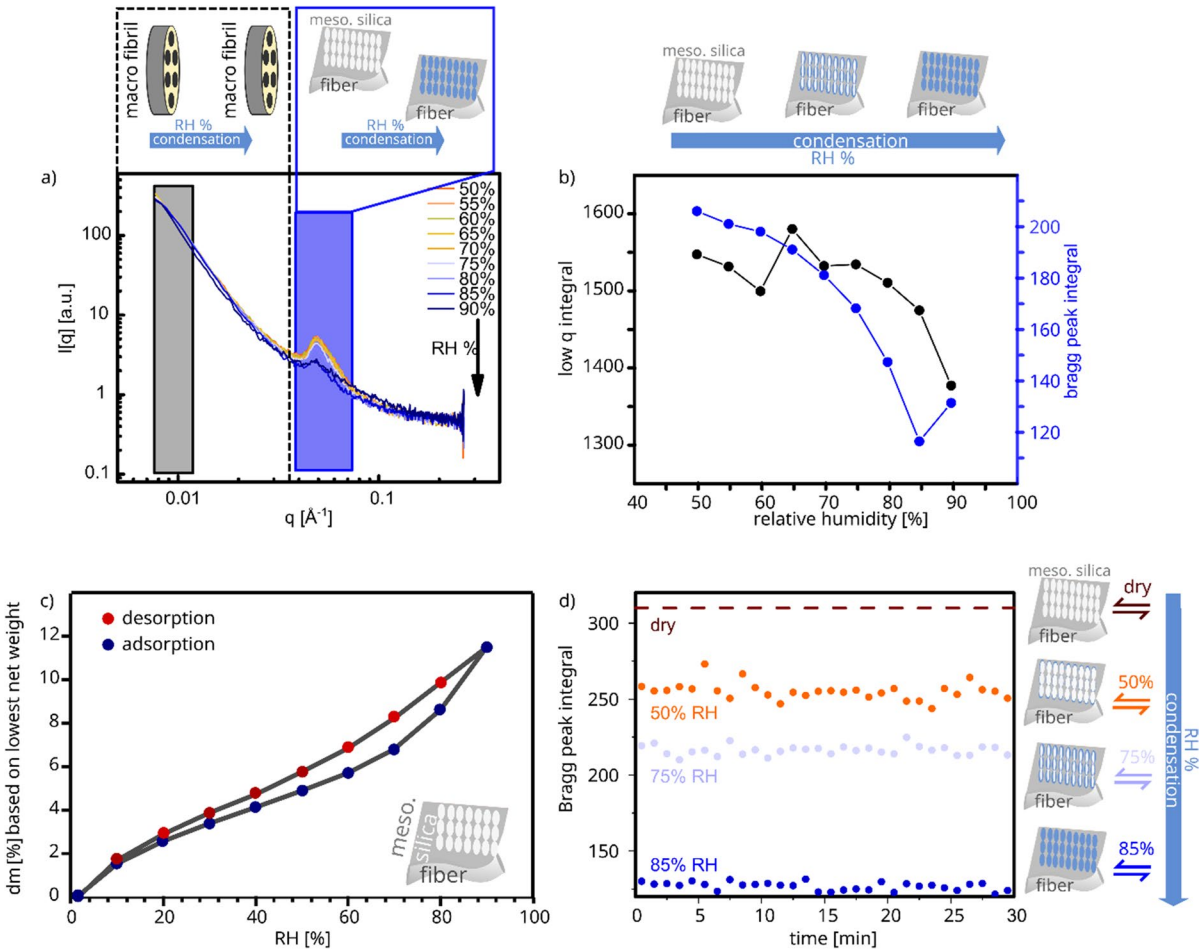

Fig. 5 **a**) SAXS measurements of mesoporous silica coated cotton linter paper which were exposed to relative humidity in a range of 50% to 90% in 5% steps. The areas, which were taken for the integrals are highlighted with a black and a blue box and plotted in dependence of the relative humidity in **b**). **c**) Water vapor adsorption (red circles) and desorption (blue circles) isotherms in the range of 0% to 90% relative humidity for mesoporous silica coated cotton linter paper. d) integrals below the Bragg peak of SAXS measurements taken at dry condition and at 50%, 75% and 85% relative humidity every one minute

Conclusion

Using SAXS and water vapor adsorption measurements mechanistic insights into wetting, drying, and water condensation in cotton linter paper with and without dense and mesoporous silica functionalization was obtained. Using SAXS, three types of water were detected: so-called 'free-water', located in the fiber–fiber voids, in the macrofibrils between the microfibrils. and is present in unmodified, dense and in mesoporous silica modified cotton linter paper sheets; so-called 'bound-water', which interacts with the cellulose polymer and which could not be detected in dense silica modified cotton linter paper; finally, 'mesopore-water', detected in mesoporous silica functionalized cotton linter paper. 'Mesopore-water' is located within the silica mesopores as indicated by changes in the Bragg peak. 'Free-' as well as 'bound-water' are present in unmodified cotton linter paper when they are in contact with liquid water. In the dense silica coated paper only 'free-water' exists which is attributed to the shielding effect of the coating which prevents the penetration of water molecules into the fiber. In mesoporous silica functionalized cotton linter paper, all three types of water are present. Furthermore, the type of water present and the hierarchical paper structure influences the drying process.

Firstly, the so-called 'free-water' evaporates. Secondly, the so-called 'bound-' and 'mesopore water' evaporates. Consequently, a two-step drying process is observed for wetted unmodified and mesoporous silica functionalized cotton linter paper. For dense silica coated paper sheets water is not able to penetrate the cotton linter fiber and thus only 'free-water' is present resulting in a one-step drying process.

Water vapor adsorption experiments performed gravimetrically as well as using SAXS measurements show a water uptake and the filling of the mesoporous inside of the silica coating due to water vapor absorption at different relative humidity. Thereby no 'free-' or 'bound-water' was detected as for liquid water contact in unmodified, dense, and mesoporous silica coated cotton linter paper, even when being deposited under high relative humidity of 95% overnight. Starting from a relative humidity of 50% water condenses into the silica mesopores up to pore filling and thus so-called 'mesopore-water' is generated.

Consequently, the local water distribution can be tuned by the silica coating and the relative humidity. In addition, liquid water can be generated into mesoporous silica coated paper even if only in contact with water vapor by using the effect of water vapor condensation in nanoscale pores. The gained insights on water distribution and especially the possibility of binding liquid water upon water condensation in mesopores of mesoporous silica coated paper sheets offers fully new possibilities in the context of paper as a construction and food packaging or as an actuator using moisture as external stimulus-trigger.

Acknowledgements The author would like to thank Christiane Helbrecht and Prof. S. Schabel (Technische Universität Darmstadt/PMV) for the support with refining the fiber material and the paper production process. In addition, the authors thank Prof. O. Azzaroni for the opportunity to work in his research group at INIFTA in La Plata Argentina.

Author contributions J.M. conducted the experiments, analyzed data, wrote the manuscript.

M.C. supervised SAXS experiments and related data evaluation and Figure generation together, Manuscript section writing with J.M. in INIFTA, La Plata, Argentina.

M.B. supported the discussion related to paper and provided access to equipment for paper fabrication.

AAB wrote the project proposal, secured funding, supervised the PhD thesis of J.M., supported experiment design, data evaluation, figure design, manuscript writing all authors reviewed the manuscript.

Funding Open Access funding enabled and organized by Projekt DEAL. The authors kindly acknowledge the financial support by the German Research Foundation (DFG) in the project AN1301/8. The SFB 1194 as well as the DAAD are acknowledged for supporting the research stay at the Instituto de Investigaciones Físicoquimicas Teóricas y Aplicadas (INIFTA-UNLAP/CONICET) in La Plata, Argentina in where the SAXS experiments were performed. MC is a staff member of CONICET Argentina. MC wants to acknowledge partial financial support from CNPEN (Brazil) under project 20220451.

Data availability The datasets and materials used in the current study are available from the corresponding author on reasonable request.

Declarations

Ethical approval Not applicable.

Conflict of interest The authors declare that they have no known competing financial interests or personal relationships that could have appeared to influence the work reported in this paper.

References

Bechtold T, Manian AP, Öztürk HB, Paul U, Siroká B, Siroký J, Soliman H, Ltt Vo, Vu-Manh H (2013) Ion-interactions as driving force in polysaccharide assembly. Carbohyd Polym 93:316–323. https://doi.org/10.1016/j.carbpol.2012.01.064

Bedane AH, Eić M, Farmahini-Farahani M, Xiao H (2016) Theoretical modeling of water vapor transport in cellulose-based materials. Cellulose 23:1537–1552. https://doi.org/10.1007/s10570-016-0917-y

Bordenave N, Grelier S, Pichavant F, Coma V (2007) Water and Moisture Susceptibility of Chitosan and Paper-Based Materials: Structure-Property Relationships. J Agric Food Chem 55:9479–9488. https://doi.org/10.1021/jf070595i

Chen W, Sun B, Biehl P, Zhang K (2022) Cellulose-Based Soft Actuators. Macromol Mater Eng 307:2200072. https://doi.org/10.1002/mame.202200072

Dano ML, Bourque JP (2009) Deformation behavior of paper and board subjected to moisture diffusion. Int J Solids Struct 46:1305–1316. https://doi.org/10.1016/j.ijsolstr.2008.10.035

Heikkinen S, Alvila L, Pakkanen TT, Saari T, Pakarinen P (2006) NMR imaging and differential scanning calorimetry study on drying of pine, birch, and reed pulps and their mixtures. J Appl Polym Sci 100:937–945. https://doi.org/10.1002/app.23051

Jayme G (1944) Mikro-Quellungsmessungen an Zellstoff. Wochenblatt Papierfabrik 6:187–194

Jayme G, Hunger G (1956) Verhornungserscheinungen an Cellulosefaserstrukturen in elektronenoptischer Sicht. Monatshefte Für Chemie Und Verwandte Teile Anderer Wissenschaften 87:8–23. https://doi.org/10.1007/BF00903586

Kaewnopparat S, Sansernluk K, Faroongsarng D (2008) Behavior of freezable bound water in the bacterial cellulose produced by Acetobacter xylinum: An approach using thermoporosimetry. AAPS PharmSciTech 9:701–707. https://doi.org/10.1208/s12249-008-9104-2

Klemm D, Heublein B, Fink HP, Bohn A (2005) Cellulose: faszinierendes Biopolymer und nachhaltiger Rohstoff. Angew Chem 117:3422–3458. https://doi.org/10.1002/ange.200460587

Larsson PT, Stevanic-Srndovic J, Roth SV, Söderberg D (2022) Interpreting SAXS data recorded on cellulose rich pulps. Cellulose 29:117–131. https://doi.org/10.1007/s10570-021-04291-x

Lee M, Kim S, Kim HY, Mahadevan L (2016) Bending and buckling of wet paper. Phys Fluids 28:042101. https://doi.org/10.1063/1.4944659

Li H, He Y, Yang J, Wang X, Lan T, Peng L (2019) Fabrication of food-safe superhydrophobic cellulose paper with improved moisture and air barrier properties. Carbohydr Polym 211:22–30. https://doi.org/10.1016/j.carbpol.2019.01.107

Li T, Chen C, Brozena AH, Zhu JY, Xu L, Driemeier C, Dai J, Rojas OJ, Isogai A, Wagberg L, Hu L (2021) Developing fibrillated cellulose as a sustainable technological material. Nature 590:47–56. https://doi.org/10.1038/s41586-020-03167-7

Liu Y, Shang S, Mo S, Wang P, Yin B, Wei J (2021) Soft actuators built from cellulose paper: A review on actuation, material, fabrication, and applications. J Sci: Adv Mater Dev 6:321–337. https://doi.org/10.1016/j.jsamd.2021.06.004

Lovikka VA, Khanjani P, Väisänen S, Vuorinen T, Maloney TC (2016) Porosity of wood pulp fibers in the wet and highly open dry state. Microporous Mesoporous Mater 234:326–335. https://doi.org/10.1016/j.micromeso.2016.07.032

Lovikka VA, Rautkari L, Maloney TC (2018) Changes in the hygroscopic behavior of cellulose due to variations in relative humidity. Cellulose 25:87–104. https://doi.org/10.1007/s10570-017-1570-9

Ma T, Inagaki T, Tsuchikawa S (2020) Rapidly visualizing the dynamic state of free, weakly, and strongly hydrogen-bonded water with lignocellulosic material during drying by near-infrared hyperspectral imaging. Cellulose 27:4857–4869. https://doi.org/10.1007/s10570-020-03117-6

Martínez-Sanz M, Gidley MJ, Gilbert EP (2015) Application of X-ray and neutron small angle scattering techniques to study the hierarchical structure of plant cell walls: A review. Carbohydr Polym 125:120–134. https://doi.org/10.1016/j.carbpol.2015.02.010

Mikolei JJ, Neuenfeld L, Paech S, Langhans L, Biesalski M, Meckel T, Andrieu-Brunsen A (2022) Mechanistic Understanding and Three-Dimensional Tuning of Fluid Imbibition in Silica-Coated Cotton Linter Paper Sheets. Adv Mater Interfaces 9:2200064. https://doi.org/10.1002/admi.202200064

Mikolei JJ, Richter D, Pardehkhorram R, Helbrecht C, Schabel S, Meckel T, Biesalski M, Ceolin M, Andrieu-Brunsen A (2023) Nanoscale pores introduced into paper via mesoporous silica coatings using sol-gel chemistry. Nanoscale 15:9094–9105. https://doi.org/10.1039/D3NR01247F

Nakamura K, Hatakeyama T, Hatakeyama H (1981) Studies on Bound Water of Cellulose by Differential Scanning Calorimetry. Text Res J 51:607–613. https://doi.org/10.1177/004051758105100909

Ogiwara Y, Kubota H, Hayashi S, Mitomo N (1970) Temperature dependency of bound water of cellulose studied by a high-resolution NMR spectrometer. J Appl Polym Sci 14:303–309. https://doi.org/10.1002/app.1970.070140204

Penttilä PA, Rautkari L, Österberg M, Schweins R (2019) Small-angle scattering model for efficient characterization of wood nanostructure and moisture behavior. J Appl Crystallogr 52:369–377. https://doi.org/10.1107/S1600576719002012

Ryu J, Mohammadifar M, Tahernia M, Chun H, ill, Gao Y, Choi S, (2020) Paper Robotics: Self-Folding, Gripping, and Locomotion. Adv Mater Technol 5:1901054. https://doi.org/10.1002/admt.201901054

Samyn P (2013) Wetting and hydrophobic modification of cellulose surfaces for paper applications. J Mater Sci 48:6455–6498. https://doi.org/10.1007/s10853-013-7519-y

Shi W, Bai H, Cao M, Wang X, Ning Y, Li Z, Liu K, Jiang L (2023) Unidirectional Moisture Delivery via a Janus Photothermal Interface for Indoor Dehumidification: A Smart Roof. Advanced Science 10:2301421. https://doi.org/10.1002/advs.202301421

Sinquefield S, Ciesielski PN, Li K, Gardner DJ, Ozcan S (2020) Nanocellulose Dewatering and Drying: Current State and Future Perspectives. ACS Sustain Chem Eng 8:9601–9615. https://doi.org/10.1021/acssuschemeng.0c01797

Venkatesan S, Afroz M, Navaratnam S, Gravina R (2023) Circular-Economy-Based Approach to Utilizing Cardboard in Sustainable Building Construction. Buildings 13:181. https://doi.org/10.3390/buildings13010181

Weise U, Maloney T, Paulapuro H (1996) Quantification of Interaction of Water in Different States with Wood Pulp Fibres. Cellulose 3:189–202. https://doi.org/10.1007/BF02228801

Zhu H, Jia Z, Chen Y, Chen Y, Weadock N, Wan J, Vaaland O, Han X, Li T, Hu L (2013) Tin Anode for Sodium-Ion Batteries Using Natural Wood Fiber as a Mechanical Buffer

and Electrolyte Reservoir. Nano Lett 13:3093–3100. https://doi.org/10.1021/nl400998t

Zhu S, Kumar Biswas S, Qiu Z, Yue Y, Fu Q, Jiang F, Han J (2023) Transparent wood-based functional materials via a top-down approach. Prog Mater Sci 132:101025. https://doi.org/10.1016/j.pmatsci.2022.101025